IEEE Access
Multidisciplinary | Rapid Review | Open Access Journal

Date of publication xxxx 00, 0000, date of current version xxxx 00, 0000.

Digital Object Identifier 10.1109/ACCESS.2017.Doi Number

Trip-Oriented Model Predictive Energy Management Strategy for Plug-in Hybrid Electric Vehicles

ZHENZHEN LEI[1, 2], (Member, IEEE), DONGYE SUN[2], JUNJUN LIU[2], DAQI CHEN[2], YONGGANG LIU[2*], (Senior Member, IEEE), ZHENG CHEN[3*], (Senior Member, IEEE)

[1]School of Mechanical and Power Engineering, Chongqing University of Science & Technology 401331, Chongqing China
[2]State Key Laboratory of Mechanical Transmissions & School of Automotive Engineering, Chongqing University, Chongqing, 400044, China
[3]Faculty of Transportation Engineering, Kunming University of Science and Technology, Kunming, Yunnan, 650500, China

Corresponding author: Zheng Chen (chen@kmust.edu.cn) and Yonggang Liu (andylyg@umich.edu).

This work was supported in part by the National Natural Science Foundation (No. 51775063 and No. 61763021), in part by the National Key R&D Program of China (No. 2018YFB0104000 and No. 2018YFB0104900), in part by the Fundamental Research Funds for the Central Universities (No. 2018CDQYQC0035), in part by the Science Foundation of Chongqing University of Science and Technology (No. CK2017ZKYB023 and No. JX2018A01), and in part by the EU-funded Marie Skłodowska-Curie Individual Fellowships Project under Grant 845102-HOEMEV-H2020-MSCA-IF-2018.

ABSTRACT Energy management strategies play a critical role in performance optimization of plug-in hybrid electric vehicles (PHEVs). In order to attain effective energy distribution of PHEVs, a predictive energy management strategy is proposed in this study based on real-time traffic information. First, an exponentially varied model for the velocity prediction is established, of which the tunable decay coefficient is regulated by the supported vector machine (SVM). In this manner, the prediction precision is improved. Then, by properly simplifying the powertrain model, the state of charge (SOC) reference trajectory is generated based on the fast dynamic programming (DP) with fast calculation speed and consideration of the traffic information. Moreover, the typical DP algorithm is leveraged to solve the nonlinear rolling optimization problem for minimizing the operating cost in a receding horizon. Simulation results demonstrate that the proposed algorithm can reach 92.83% operating savings, compared with that of the traditional DP; and save 6.18% cost compared with the MPC algorithm only with reference of the trip duration.

INDEX TERMS plug-in hybrid electric vehicles (PHEVs); energy management; model predictive control (MPC); traffic information; state of charge (SOC) reference

I. INTRODUCTION

Nowadays, transportation electrification paves a potential way to mitigate air pollution and decrease greenhouse gas (GHG) emission [1, 2]. Hybrid electric vehicles (HEVs), as a combination of traditional internal combustion engine (ICE) driven vehicles and pure electric vehicles (EVs), usually employ an ICE together with a battery pack to supply the driving energy [3]. Thus, an energy distribution problem arises due to existence of two sources [4]. Plug-in HEVs, which can be charged from the power grid, not only inherit all advantages of HEVs, but also can supply a certain all-electric range (AER) [5]. Similarly, it is equally important to allocate the energy distribution of PHEVs between the engine and battery properly, referred to as energy management strategies (EMSs), thereby improving their fuel economy and extending the battery lifespan [5, 6].

Currently, EMSs have been widely researched by industry and academia. In general, EMSs can be mainly divided into two categories, i.e., rule-based algorithms and optimization-based algorithms [7]. Rule-based algorithms are comprised of one or more rule tables with inputs of the vehicle speed, acceleration, battery state of charge (SOC), etc. and outputs of the torque of the engine and motor [8]. Generally, rule-based EMSs can be classified into determined rule strategies and fuzzy rule strategies [9]. In [10], the EMS based on deterministic rules and fuzzy logic are discussed to compare their pros and cons, respectively. The main goal of rule-based EMSs is to keep the power sources working in their high efficiency region, thus

improving the fuel economy and reducing emissions to some extent. The rule-based strategy is generally robust, reliable and efficient; nonetheless, the design of rules inside the strategy require substantial experience, repetitive calibration and trial-and-error iteration [11]. Moreover, it is difficult to take emerging environmental information such as the driver's habit and transportation information into account.

As a consequence, optimization-based algorithms begins to attract attention since energy management of PHEVs is essentially a high nonlinear sequential optimal decision problem [12]. Typical optimal control theories have already been widely researched and applied to energy management with different targets. They can be mainly classified into two types, i.e., global optimal solutions and local optimal algorithms [13]. Among all global optimal strategies, dynamic programming (DP) and Pontryagin's minimum principle (PMP) are the most popular candidates [14]. Ref. [15] considers the total fuel consumption of a PHEV as the objective function for optimization and adopts DP to solve it. Ref. [16] takes the impact of different powertrain structures into account and employs DP to evaluate the fuel economy of vehicles with P1 and P2 configuration. In [17], two cost functions are established by considering simultaneous optimization of the battery life and fuel consumption, and finally a multi-mode switching strategy is built. In [18], DP is employed to optimize the battery current to reduce the fuel consumption. PMP can theoretically find optimal solutions for energy allocation of PHEVs by solving the Hamilton function, including the target function, related constraints and vehicle powertrain model expressed by simplified linear or nonlinear functions [19]. In [20], the PMP is exploited to optimize the speed curve and power distribution in real-time to achieve lowest fuel consumption according to the future traffic flow. In [21], the optimal reference SOC trajectory is found by the PMP under different driving conditions, which provides a solid theoretical basis for designing rule-based strategies. In [22], PMP is leveraged to obtain the optimal fuel consumption with knowing the driving cycle *a priori*, and the solutions are considered as the foundation of the real time controller. However, a main constraint when applying DP and PMP is that the whole driving condition should be acquired in advance, leading to impossibility and difficulty of online application [23-25]. From this point of view, global optimization solution calculated by DP and PMP is generally regarded as a reference or benchmark for examining performance of other strategies [26].

Local optimal control strategies often declare to find suboptimal, or even optimal, solutions by immediate calculation according to the current vehicle status. Typical representatives include the equivalent consumption minimization strategy (ECMS) [27] and model predictive control (MPC) algorithm [28]. For the former, the key task is to find an appropriate equivalent factor which is usually determined by experience or optimal theories in the light of the road condition, battery status and power demand [29]. Currently, adaptive and predictive ECMSs are actively researched [30]. While for the latter, it is critical to design an effective control reference curve, usually the battery SOC trajectory, which keeps challenging and needs to be carefully tackled by incorporating the road information and vehicle status [31]. Nowadays, fusion algorithms that combine rule-based and optimization-based strategies have been put forward, trying to absorb both advantages and consequently improving controlling performances [23, 32]. Ref. [21] introduces a fusion algorithm based on the fuzzy logic control and ECMS, and simulation results reveal the feasibility of reducing the fuel consumption. In [28], the DP is leveraged to find the optimal working region of engine in a PHEV, and rules are excavated from offline optimal results. In [33], the driving-mode transition and gear shifting rules are extracted by DP, and then the ECMS is applied together with those rules to conduct effective torque distribution between the engine and motor. Simulation results manifest that these rules can be implemented in real-time with superior savings of the fuel consumption. Ref. [34] calculates the equivalent factor with a causal adaption law in the ECMS framework to improve the fuel economy in hilly driving conditions. MPC is an effective method to deal with process control problems with multi inputs and outputs together with different constraints [35]. It has also been widely applied in energy management of PHEVs [36]. In [37], the EMS is proposed based on a bi-level MPC, and it can effectively solve the optimal torque distribution and gear shift and moreover design the velocity trajectory for HEVs. Ref. [26] presents a strategy by incorporating DP and PMP to solve a five state mixed-integer energy management problem, and this method exhibits the same controlling quality with DP with faster calculation speed. In [38], a projected interior point method is considered to realize the nonlinear MPC of energy management of a HEV. In [39], the vehicle to vehicle (V2V) and vehicle to infrastructure are referred to predict the preceding vehicle movement and road terrain profile, and on the basis of the predicted information, a nonlinear MPC is proposed to reduce the energy consumption. In [40], the sequential quadratic programming (SQP) is employed to solve the rolling optimization in the MPC framework. Simulation results indicate that the strategy outperforms the rule based strategy with little trip information.

Actually, when applying MPC, three critical aspects should be carefully considered including establishment of the prediction model, design of the controlling reference, and implementation of rolling optimization [41]. With respect to applications in energy management of PHEVs, common manners of building the prediction model include the Markov chain [42], neural networks (NNs) [43], and exponentially varying prediction [44]. In [45], the short-term historical speed data is trained based on the back

This article has been accepted for publication in a future issue of this journal, but has not been fully edited. Content may change prior to final publication. Citation information: DOI 10.1109/ACCESS.2019.2933015, IEEE Access

propagation NN (BPNN) to predict the future velocity. In [46], a multi-step Markov chain is built to predict future driving conditions. Ref. [47] compares the prediction effects of driving speed conducted by the exponentially varying prediction, Markov chain and NN, and reveals that the prediction accuracy can be affected by types of driving conditions to a large extent. In [48], the Markov chain is implemented to learn driving behaviors online, which are subsequently imported into the stochastic MPC. Through principal component analysis (PCA) and cluster analysis of historical condition information, a real-time prediction model is established based on the Markov chain to forecast future speed in a varied duration [49]. In [30], a NN model is built to predict the velocity in a short term according to the historical data. Actually, exponentially varying prediction algorithms are widely adopted for the velocity prediction in MPC due to their simplicity and low computation intensity [50, 51]. As the name implies, it employs a simple exponentially varying function to predict future information in a receding horizon. The exponentially varying predictor was firstly leveraged to facilitate the MPC to be applied in energy management of HEVs in [52]. In [53], an exponentially varying prediction model is built to predict the torque demand in a short-term period, and then the velocity is forecasted according to the predicted torque. Ref. [30] manifests that the prediction accuracy of the exponentially varying model exerts a certain impact on fuel economy improvement of HEVs. Ref. [54] details the MPC application for energy allocation of HEVs based on exponentially varying velocity prediction, of which the decay coefficient is dynamically tuned on basis of the diving information. How to devise an adaptive strategy to regulate the decay coefficient according to the driving condition, to the best of authors' knowledge, is seldom reported.

In addition, to implement MPC, it is necessary to develop a suitable reference curve, usually the reference SOC trajectory, for energy management of PHEVs during the entire process [45]. By analyzing planning algorithms of the reference SOC trajectory in existing literatures, we summarize that they are mainly divided into two categories. One is to apply global optimization algorithms to plan it according to the historical working condition [55], and the other is to design it simply only according to the driving range or duration [56]. To the best of authors' knowledge, there are few studies on the SOC trajectory planning on basis of real-time updated traffic information. For PHEVs, it is ideal to use up all allowable energy stored in battery when the vehicle reaches destination, and thus the operating cost can be minimized because of lower price of electricity. In the MPC framework, the SOC reference should be planned in advance ahead of departure [57]. In [46, 58], the SOC reference is supposed to linearly decrease with trip duration, based on which the research declares that the MPC gains less fuel consumption, compared with the traditional ruled based strategy under Chinese typical urban cycle. In [59, 60], the SOC reference trajectory within the prediction itinerary is constructed based on the optimal depth of discharge. Assuming that only the travelling distance or duration is known, previous research has demonstrated effectiveness of the SOC reference that linearly changes with distance or duration [56]. However, its effect cannot be competitive with that solved by DP, since the latter one is obviously not a linear or piecewise linear function with respect to driving distance or duration due to the time-varied velocity and power demand. To overcome this drawback, determination of the SOC reference should fully consider historical and current transportation information. How to effectively integrate real-time transportation information to assist generation of the SOC reference trajectory remains further investigated. Ref. [61] constructs a simple power-based model to generate the SOC reference trajectory and optimizes it according to the route information and real-time traffic data. Refs. [62, 63] propose an economic driving principle which fully considers real-time traffic information to assist determination of the reference SOC trajectory.

Inspired by the discussions mentioned above, we conclude that a predictive control framework with full incorporation of traffic information should be able to achieve superior energy management of PHEVs with real-time application. This becomes the main motivation of our research. In this study, an MPC control framework is constructed including the fast SOC reference that is solved by DP with real-time updated traffic information, and the future speed prediction implemented by an exponentially varied algorithm. In the speed prediction algorithm, the decay coefficient is dynamically regulated by the support vector machine (SVM) according to the road type. Numerous simulations validate that the proposed control framework is feasible to save the operating cost according to the real-time traffic information.

The main contribution of this paper can be attributed to the following three aspects. First of all, a uniform control framework is proposed by integrating the long-term planning and short-term prediction, and the rules of extracting the traffic information are investigated for application in MPC. Secondly, by constructing the traffic model, an algorithm to study the traffic information is provided, thus paving the road for applying the proposed predictive EMS in real condition. Meanwhile, the real-time transportation information is bridged to the MPC framework to further reduce the vehicle operating cost. Thirdly, a fast DP is employed to find the global SOC reference with satisfactory calculation speed.

The rest of this article is structured as follows. The vehicle modeling and predictive EMS framework are detailed in Section II. The exponentially varying prediction model is proposed in Section III; and the decay coefficients identification is illustrated in Section IV. The reference

SOC trajectory and rolling optimization are explained in Section V, followed by the simulation validation and discussion presented in Section VI. Finally, main conclusions are drawn in Section VII.

II. MPC-BASED ENERGY MANAGEMENT FOR PHEV

A. The PHEV Configuration

In this paper, a parallel PHEV is chosen as the research target, of which the configuration is structured in Fig. 1. As can be seen, the hybrid powertrain system includes an engine, an integrated starter generator (ISG) motor, a main clutch, a battery pack and a dual clutch transmission (DCT). In addition, the engine control unit (ECU), battery management system (BMS) and vehicle control unit (VCU) are also indispensable to facilitate control of the vehicle powertrain. The functions of the clutch and DCT are to switch the driving modes and to regulate the output ratio of the torque and speed according to the driving power demand. The driving resistance of the vehicle is shown in Fig. 2. The demanded torque and speed of the vehicle can be calculated, as:

$$\begin{cases} T_w = (mg\sin\alpha + f_r mg\cos\alpha + \dfrac{\rho_a}{2} C_D A v^2 + \delta m \dfrac{dv}{dt}) \cdot r_w \\ \omega_w = \dfrac{v}{r_w} \end{cases} \quad (1)$$

where v is the vehicle velocity, ρ_a denotes the air density, r_w expresses the radius of wheels, ω_w means the wheel rotating speed, T_w indicates the torque demand, A denotes the frontal area, C_D is the aerodynamic drag coefficient, f_r expresses the rolling resistance coefficient, m is the vehicle mass, δ is the total vehicle rotational inertia coefficient, and α is the slope information. Main parameters are listed in Table I.

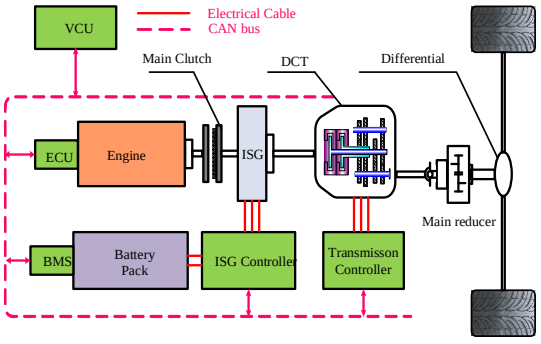

FIGURE 1. The configuration of the PHEV.

To simplify the optimization problem, the dynamic characteristics of the hybrid powertrain is not considered in this study. On this basis, a quasi-static methodology is employed to model the powertrain, as:

$$\dot{m}_{fuel} = \psi_1(n_e, T_e) \quad (2)$$

$$\eta_m = \psi_2(n_m, T_m) \quad (3)$$

where ψ_1 and ψ_2 denote the empirical fuel rate map with unit of g/Kwh and the efficiency of ISG, respectively. Similar to [24], an equivalent circuit model shown in Fig. 3 that consists of an open circuit voltage source and a resistor connected in series, is implemented to characterize the electrical performance of the battery with advantages of simple computation and acceptable precision. Easily, the battery current and SOC derivation can be calculated as:

$$\begin{cases} I = \dfrac{V_{oc}(SOC) - \sqrt{V_{oc}(SOC)^2 - 4R_{batt}(SOC)P_{batt}}}{2R_{batt}(SOC)} \\ \dfrac{dSOC}{dt} = -\dfrac{V_{oc} - \sqrt{V_{oc}^2 - 4(P_{batt})R_{batt}}}{2Q_{batt}R_{batt}} \end{cases} \quad (4)$$

where I is the current of battery, $V_{oc}(SOC)$ and $R_{batt}(SOC)$ denote the open circuit voltage and internal resistance with respect to SOC, and Q_{batt} means the battery capacity.

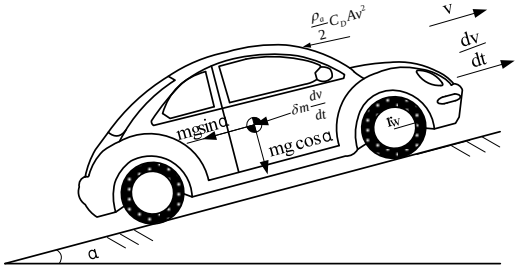

FIGURE 2. The driving resistance of the PHEV.

TABLE I
BASIC PARAMETERS OF PHEV

Parameter	Nomenclature	Value
Vehicle Mass	m	1350 kg
Frontal area	A	2.228 m^2
Aerodynamic drag coefficient	C_D	0.32
Wheel radius	r_w	0.295 m

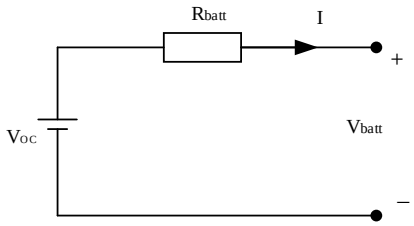

FIGURE 3. The battery equivalent circuit model.

B. Predictive Energy Management Strategy

In this study, the algorithm acquires the traffic information in real time according to actual position of the vehicle and updates it in a traffic environment with a fixed frequency. Based on it, the SOC reference trajectory is planned and updated with a fast calculation speed, and the short-term future speed is predicted. Then, the MPC is applied to achieve the energy management of the vehicle. The detailed control framework is sketched in Fig. 4 and calculation procedures are listed as follows.

This article has been accepted for publication in a future issue of this journal, but has not been fully edited. Content may change prior to final publication. Citation information: DOI 10.1109/ACCESS.2019.2933015, IEEE Access

1) The future velocity and acceleration are predicted at step *k* through the exponentially varying prediction model based on the driving cycle recognition;
2) The real-time traffic information in the route is updated to generate the SOC reference;
3) The optimal controlling sequence is calculated by the MPC controller within the prediction horizon and with the help of predicted velocity and SOC reference;
4) The first output of the controlling sequence is applied, and simultaneously the vehicle state is updated;
5) Repeat steps 1) to 4) until the end of trip.

In this study, an exponentially varying prediction model is established together with an adaptively adjusted decay factor to predict the future velocity according to the traffic information. In addition, a fast DP algorithm is applied to generate the SOC reference with fast speed to ensure both real-time implementation and acceptable accuracy.

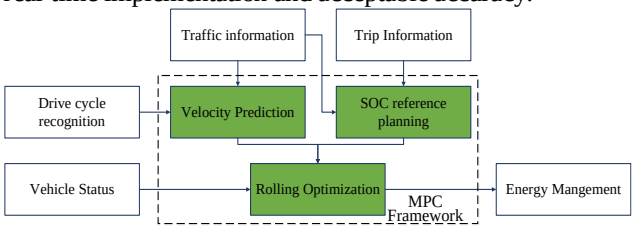

FIGURE 4. **Framework of the MPC-based control strategy.**

III. EXPONENTIALLY VARYING PREDICTION MODEL

A. Exponentially Velocity Prediction

Essentially, the exponentially varying prediction model operates by assuming the vehicular velocity and acceleration would vary exponentially in a prediction horizon. Thus, the following equations can be attained:

$$\begin{cases} a_{pre}(k+i) = a(k)\cdot\exp(-\dfrac{i}{T_d}) \\ v_{pre}(k+i) = a_{pre}(k+i) + v_{pre}(k+i-1) \end{cases} \quad i = 1,2,...,p \quad (5)$$

where $a_{pre}(k+i)$ and $v_{pre}(k+i)$ denote the predicted acceleration and velocity at step $k+i$, $a(k)$ is the current acceleration, T_d means the decay coefficient, and p is the length of prediction horizon. In this paper, the root mean square error (RMSE) is adopted to evaluate accuracy of the predicted velocity, as formulated in (6), and we can easily find that the prediction accuracy is inversely proportional to RMSE [64].

$$\begin{cases} RMSE(k) = \sqrt{\dfrac{1}{p}\sum_{i=1}^{p}(v(k+i) - v_r(k+i))^2} \\ RMSE = \sqrt{\sum_{k=1}^{t_{cyc}} RMSE^2(k)/t_{cyc}} \end{cases} \quad (6)$$

where $RMSE(k)$ denotes the RMSE at step *k*, t_{cyc} means the total duration, and $RMSE$ is the mean value of $RMSE(k)$ and quantifies the overall error level in the whole trip. As referred in [61], the optimal prediction horizon is limited within 6 s to 12 s. In this study, we adopted 10 s as the length of prediction horizon after trail-and-error. Correspondingly, the predicted velocity of the LA92 cycle based on the traditional exponential varying prediction model is shown in Fig. 5. As can be observed, large error may exist when the velocity faces with sudden change. A fixed decay coefficient is inappropriate to predict the velocity in the whole driving duration due to the varied road condition and different driving demand. Consequently, T_d needs to be regulated dynamically according to the road type. Since the driving cycle recognition is essentially a multi-parameter nonlinear classification problem, the SVM is suitable for solving such problems. Therefore, in this study, the SVM is implemented to conduct identification of the driving conditions, and the decay coefficient is accordingly adjusted to improve the prediction precision of the future speed.

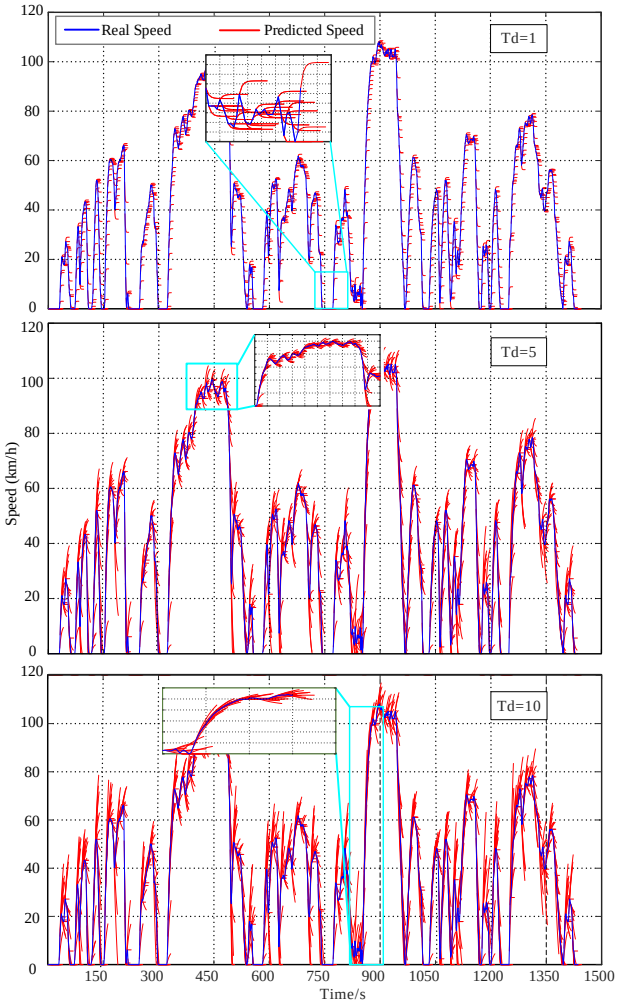

FIGURE 5. **Velocity prediction with different decay factor under LA92.**

B. Classification of the Driving Conditions Based on the SVM

SVMs declare to achieve satisfactory classification results even with limited samples [65]. Previous researches manifest that SVMs is an effective algorithm for data classification

This article has been accepted for publication in a future issue of this journal, but has not been fully edited. Content may change prior to final publication. Citation information: DOI 10.1109/ACCESS.2019.2933015, IEEE Access

and regression analysis. By referring the research in [31] and considering characteristics of the exponential varying prediction model, ten feature parameters related to the vehicular velocity are selected to identify the driving cycle, as listed in Table II.

To obtain the training samples, six typical driving cycles, i.e., NYCC, New York Bus, ECE_EUDC_LOW, UDDS, HWFET and US06_HW, are selected to represent the typical urban, suburban, and highway driving conditions, respectively. For ease of identifying the driving type, we divided the whole combination of these cycles into a number of sections, and the duration of each section is 120 s [66]. In this manner, the database is established, and the identification of the decay factor is conducted as follows.

1) Divide the standard driving cycle into 140 sample datasets with each duration of 120 s;
2) Calculate the characteristic parameters for each dataset and the RMSE when T_d changes from 1 to 10, and select T_d when the RMSE reaches the minimum value as the optimal decay coefficient of the selected dataset;
3) Classify all the dataset into 10 categories according to the difference among T_d.

TABLE II
FEATURE PARAMETERS

Feature Parameter	Expression
maximum speed $v_{\max}$	$v_{\max} = \max(v_g)$
average speed $\bar{v}$	$\bar{v} = \frac{1}{t_g}\sum_{i=1}^{t_g} v_g$
maximum acceleration $a_{\max}$	$a_{\max} = \max(a_g)$
average acceleration $\bar{a}$	$\bar{a} = \frac{1}{t_g}\sum_{i=1}^{t_g} a_g$
maximum deceleration $d_{\max}$	$d_{\max} = \max(d_g)$
average deceleration $\bar{d}$	$\bar{d} = \frac{1}{t_g}\sum_{i=1}^{t_g} d_g$
idling factor r_i	$r_i = t_i / t_{cyc}$
acceleration factor r_a	$r_a = t_a / t_{cyc}$
deceleration factor r_d	$r_d = t_d / t_{cyc}$
uniform speed factor r_c	$r_c = t_u / t_{cyc}$

The principle of SVM is to transform the nonlinear input space into high-dimensional or infinite-dimensional feature space, and find a dividing hyperplane with the largest margin to separate training sample set belonging to different categories, which can be expressed as:

$$D = \{(x_1, y_1), (x_2, y_2), \cdots (x_n, y_n)\} \tag{7}$$

where $n = 125$ represents the number of the training samples; x expresses the input vector and equals $\{v_{\max}, \bar{v}, a_{\max}, \bar{a}, d_{\max}, \bar{d}, r_i, r_a, r_d, r_c\}$; and y means the driving condition type, $y = \{1,2,3,4,5,6,7,8,9,10\}$. In the feature space, the model of the hyperplane can be described as:

$$y = w^T \phi(x) + b \tag{8}$$

where $w = \{w_1; w_2; \cdots; w_d\}$ is the normal vector of the hyperplane, which determines the direction; $\phi(x)$ is the feature vector of the original input vector mapping to the high dimensional space; and b is a real number, which determines the distance between hyperplane and origin. Based on the hyperplane model, the distance from two heterogeneous support vectors to the hyperplane can be calculated as:

$$\gamma = \frac{2}{\|w\|} \tag{9}$$

To find the hyperplane with the maximum margin between the two heterogeneous support vectors, $\|w\|^2$ needs to be minimized, as:

$$\min_{w,b}\left(\frac{1}{2}\|w\|^2\right) \tag{10}$$

In addition, it should be subjected to

$$y_i(w^T \phi(x_i) + b) \geq 1, i = 1, 2, \cdots, n. \tag{11}$$

In general, to efficiently solve the problem similar to (10), the Lagrange multiplier method is applied to transform the problem into a dual problem. Likewise, the Lagrange multiplier is added to the constraint in (11) to formulate the dual problem, as:

$$\begin{cases} \max\limits_{\alpha} \sum\limits_{i=1}^{m} \alpha_i - \frac{1}{2}\sum\limits_{i=1}^{m}\sum\limits_{j=1}^{m} \alpha_i \alpha_j y_i y_j \phi(x_i^T)\phi(x_j) \\ s.t. \begin{cases} \sum\limits_{i=1}^{m} \alpha_i y_i = 0, \\ \alpha_i \geq 0, i = 1, 2, \cdots, n. \end{cases} \end{cases} \tag{12}$$

where $\phi(x_i^T)\phi(x_j)$ is the inner product of x_i and x_j mapped to the feature space. Since the dimension of the feature space may be quite large, it is difficult and even impossible to calculate it directly. Therefore, the kernel function $k(x_i, x_j) = \phi(x_i^T)\phi(x_j)$ is introduced to overcome this restriction. Now, the optimal solution of the hyperplane model turns into the kernel function of the training sample, as:

$$f(x) = w^T \phi(x) + b = \sum_{i=1} \alpha_i y_i k(x_i, x) + b \tag{13}$$

In this study, we chose the RBF kernel function, shown in (14), because of its strong mapping capability.

$$k(x_i, x_j) = \exp\left(-\frac{\|x_i - x_j\|^2}{2\sigma^2}\right) \tag{14}$$

where $\sigma > 0$ denotes the width of the RBF kernel function and reflects the distribution of the RBF. The smaller the value, the more concentrated the RBF distribution will be, and the higher possibility the over-fit would occur with. In real application, even the proper kernel function is found to make the training set linearly separable in the feature space, it is still difficult to judge whether the linearly separable result is caused by the overfitting. To alleviate this problem, this

This article has been accepted for publication in a future issue of this journal, but has not been fully edited. Content may change prior to final publication. Citation information: DOI 10.1109/ACCESS.2019.2933015, IEEE Access

paper introduces the soft margin that allows the SVM to generate some errors in a number of samples, which means that some training samples do not satisfy the constraint of $y_i(w^T\phi(x_i)+b)\geq 1$. The optimizing target can be expressed as:

$$\min_f \Omega(f)+C\sum_{i=1}^{n}\ell(f(x_i),y_i) \tag{15}$$

where $\Omega(f)$ represents structural risk, denoting properties of the hyperplane model; $\ell(f(x_i),y_i)$ represents the loss function; $\sum_{i=1}^{n}\ell(f(x_i),y_i)$ denotes the empirical risk that quantifies the fitting degree between the model and training data; and C is a constant for compromising $\Omega(f)$ and $\sum_{i=1}^{n}\ell(f(x_i),y_i)$, and positively correlates with complexity of the model. Larger C leads to overfitting more possibly. Due to its non-convex and non-continuous characteristics of the loss function, the hinge loss function is replaced as the alternative loss function, and the dual problem of (15) can be rewritten as:

$$\begin{cases}\max\limits_{\alpha}\sum\limits_{i=1}^{m}\alpha_i-\frac{1}{2}\sum\limits_{i=1}^{m}\sum\limits_{j=1}^{m}\alpha_i\alpha_j y_i y_j\phi(x_i^T)\phi(x_j)\\ s.t.\begin{cases}\sum\limits_{i=1}^{m}\alpha_i y_i=0,\\ 0\leq\alpha_i\leq C, i=1,2,\cdots,n.\end{cases}\end{cases} \tag{16}$$

In this paper, σ and C are validated to search the optimal values with the highest classification accuracy. The cross-validation results are shown in Fig. 6. The remaining 15 samples are considered to verify the performance and corresponding results are shown in Fig. 7. As can be seen, the accuracy is 100%, demonstrating feasibility of the SVM model.

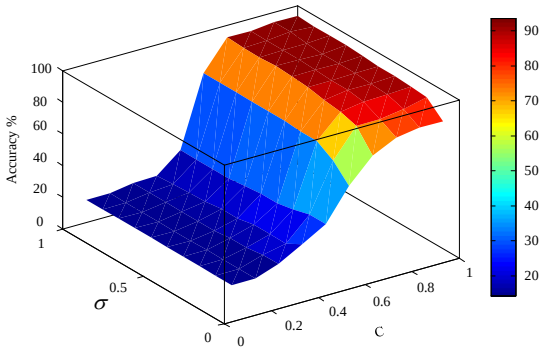

FIGURE 6. **The cross validation of recognition accuracy.**

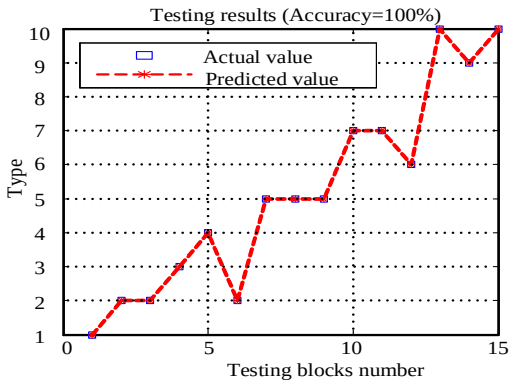

FIGURE 7. **Testing results of SVM.**

C. Exponentially Varying Prediction Model Based on the Driving Cycle Recognition

A blended driving cycle that consists of the WVUSUB, MANHATTAN, 1015, UDDS and HWFET cycles is built to verify effectiveness of the proposed prediction model. T_d is determined based on the driving speed and the recognition results are described in Fig. 8. We can find that T_d is higher when the vehicle changes dramatically and is lower when the velocity variation is flat, indicating that the proposed prediction algorithm could better identify the type of the driving block. In order to compare the prediction effects of the exponential prediction model based on the driving condition identification and the optimal fixed decay factor, the vehicle speed prediction is carried out for LA92, UDDS and the blended driving cycle, respectively. The results are shown in Table III. Even it does not improve too much, however, the baseline of 2.023 is calculated based on the optimal fixed decay factor. It seldom happens that finding the optimal fixed factor for a certain driving cycle.

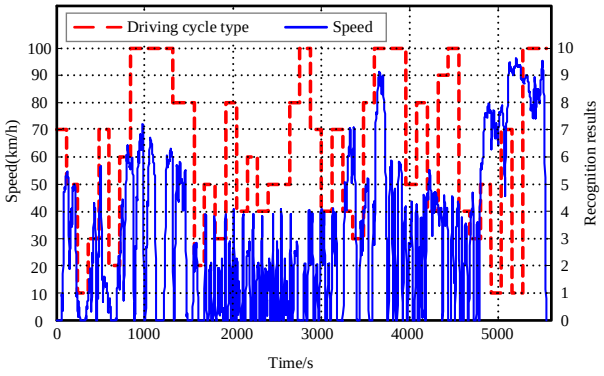

FIGURE 8. **The recognition results.**

TABLE III
RESULTS OF EXPONENTIAL PREDICTION MODEL BASED ON SVM RECOGNITION

Driving cycle	Based on SVM recognition RMSE(m/s)	Optimal fixed Td RMSE(m/s)
LA92	3.035	3.192
HWFET	1.071	1.154
Blended	1.946	2.023

This article has been accepted for publication in a future issue of this journal, but has not been fully edited. Content may change prior to final publication. Citation information: DOI 10.1109/ACCESS.2019.2933015, IEEE Access

IV. TRIP MODELING USING REAL-TIME TRAFFIC INFORMATION

To improve fuel economy and exploit operating efficiency of the battery, a global SOC reference trajectory should be designed considering the traffic information. First, the traffic environment analysis is conducted.

A. TRAFFIC ENVIRONMENT ANALYSIS

This study employed a micro traffic simulation tool, i.e. VISSIM, to simulate the transportation environment, which is widely adopted for traffic evaluation and performance assessment of energy management of HEVs [67]. The actual collected route starting from point A and terminating at point B is highlighted in green in Fig. 10 and the total distance is 26.4 Km. The driving condition in this route is diverse and complex and involves a section of urban congestion road transferring from normal driving to traffic jam and a section of highway road.

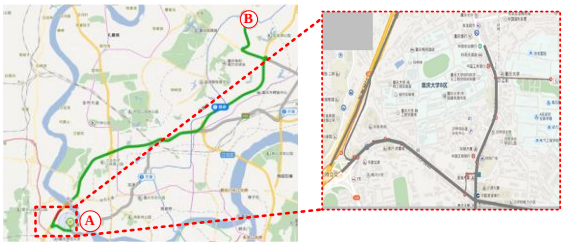

FIGURE 9. The route map of the VISSIM.

As depicted in the amplified district of Fig. 9, intersections are taken into account to simulate the urban congestion. The real-time traffic information is derived from the set road sensors. The key traffic information required in this study is the current average velocity of the upcoming trip. The selected route is divided into a number of segments with each of 200 m. In this manner, it become more convenient to collect the current average velocity of the traffic flow recorded by the road sensors at each segment. In this study, V_{seg} , representing the average velocity of each upcoming segment, is connected sequentially, and adds in VISSIM and updates every 200 s. The average traffic flow velocity can be calculated as:

$$V_{seg(\mathrm{i})} = \frac{1}{N}\sum_{k=1}^{N} V_k^{seg(\mathrm{i})} \quad (\mathrm{i} = 1, 2, ..., 132) \tag{17}$$

where $V_{seg(\mathrm{i})}$ is the average traffic flow velocity of segment i , $V_k^{seg(\mathrm{i})}$ denotes the velocity of the kth vehicle through the segment i , and N is the total number of vehicles in the segment i .

As shown in Fig. 10, the whole route information is created in VISSIM, and the traffic environment stays steady within about 3 hours. The vehicle starts from a traffic junction between 2800 s and 3000 s. After that, the vehicle speeds up and runs in the urban highway. Finally, the vehicle leaves the urban expressway and arrives at the destination.

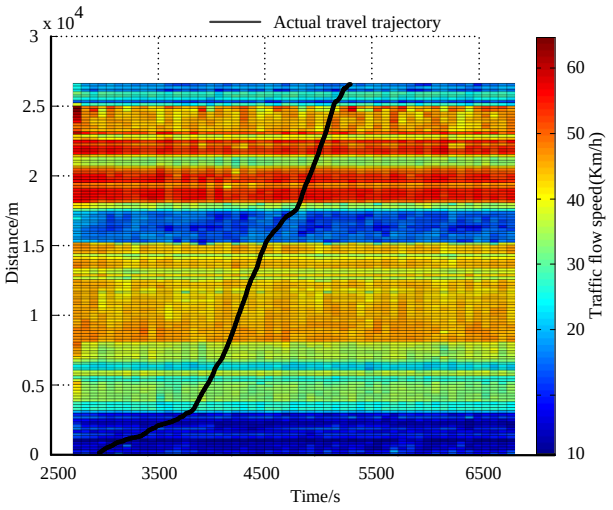

FIGURE 10. The segment average speed in the traffic environment.

B. TRIP MODELING

The purpose of the trip modeling is to generate a trackable driving cycle for the upcoming route with help of transportation information including the traffic flow speed, speed limitation and traffic lights signal. The transportation information derived from road sensors is the average speed of the traffic flow and can be integrated into the trip model by transferring the road grade from spatial domain to time domain. The travel time of each segment $T_{seg(i)}$ can be expressed as

$$T_{seg(i)} = \frac{L}{V_{seg(i)}} \tag{18}$$

where L is the length of each segment. Actually, the generated driving cycle is a staircase signal due to discrete acquired signal of speed, and thus it is infeasible when generating the SOC reference for future online control. In this study, the Butterworth filter is leveraged to produce smoother velocity profile, as shown in Fig. 11.

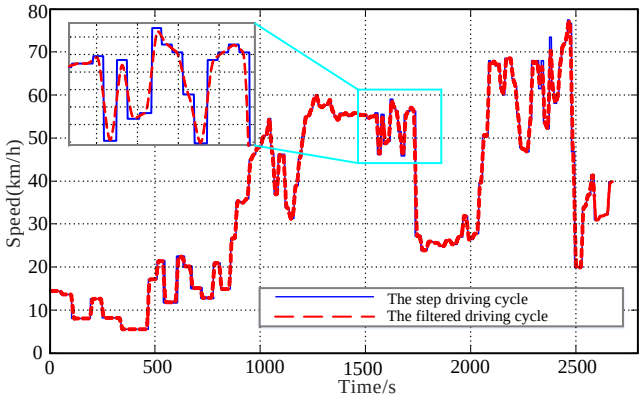

FIGURE 11. The trip model based on real time traffic data.

In the following, the generated speed profile is incorporated into the energy management controller to

This article has been accepted for publication in a future issue of this journal, but has not been fully edited. Content may change prior to final publication. Citation information: DOI 10.1109/ACCESS.2019.2933015, IEEE Access

achieve the power distribution among different energy sources. Next step, the SOC reference generation and rolling optimization is detailed for realizing the MPC application.

V. SOC REFERENCE GENERATION AND ROLLING OPTIMIZATION

A. FAST DP CONTROL METHOD

Nowadays, the DP algorithm is widely harnessed to optimally plan the SOC trajectory for a given driving cycle. However, due to large calculation intensity, the DP algorithm needs to be simplified when considering real-time traffic information. To achieve it, the following two steps are conducted to simplify the calculation process.

1) Fit the efficiency model of the engine and motor by a few quadratic equations. Traditional DP finds the corresponding fuel rate based on the characteristic map through an interpolation function. However, repetitive interpolations would certainly increase the computation complexity, which therefore leads to larger computation effort. In this study, a five-order polynomial equation is employed to simulate the relationship between the fuel rate efficiency and engine power, as

$$\eta_{tank}(P_e) = p_1 \cdot P_e^4 + p_2 \cdot P_e^3 + p_3 \cdot P_e^2 + p_4 \cdot P_e + p_5 \quad (19)$$

And the fitting coefficients p_1 to p_5, solved by the least square method, equal $-1.157e^{-07}$, $1.556e^{-05}$, $7.849e^{-04}$, 0.01751 and 0.1635, respectively.

A five-order polynomial equation is employed to simulate the relationship between the motor efficiency and motor power in the driving mode, as:

$$\begin{aligned}\eta_m(P_{m\_dis}) = {} & k_1 \cdot P_{m\_dis}^4 + k_2 \cdot P_{m\_dis}^3 \\ & + k_3 \cdot P_{m\_dis}^2 + k_4 \cdot P_{m\_dis} + k_5\end{aligned} \quad (20)$$

where the fitting coefficients k_1 to k_5, solved by the least square method, equal $-1.967e^{-06}$, $1.21e^{-04}$, -0.002862, 0.02551 and 0.7049, respectively. The Gaussian function is employed to illustrate the relationship between the motor efficiency and motor power in the regeneration mode, as:

$$\begin{aligned}\eta_m(P_{m\_chr}) = {} & a_1 \cdot exp(-((P_{m\_chr} - b_1)/c_1)^2) \\ & + a_2 \cdot exp(-((P_{m\_chr} - b_2)/c_2)^2)\end{aligned} \quad (21)$$

in which the fitting coefficients a_1, a_2, b_1, b_2, c_1 and c_2, equal 2.342, 9.688, 19.76, -3154, 12.52 and 2191, respectively.

The fitting results are shown in Fig. 12, which indicates that the polynomial equation can approximate the fuel efficiency with acceptable precision. Based on the engine power, the fuel efficiency can be determined by solving (19), and consequently the fuel power and the fuel rate can be determined. The total calculation process is illustrated in (22). Similarly, the motor efficiency is also fitted in the same manner. Corresponding results are shown in Fig. 13. According to the current power and state of the motor, the efficiency of the motor can be calculated by (20) and (21), and then the battery power can be found by (23). As such, the calculation of the fuel rate and efficiency of motor can be simplified by the corresponding equations, and thus the computation effort be dramatically reduced.

$$\begin{cases}\eta_{\text{tank}} = \dfrac{P_{\text{e}}}{P_{\text{tank}}} \\ P_e = T_{\text{e}} \times n_e / 9550 \\ P_{\text{tank}} = Q_{fuel} / g \cdot zd \cdot H_u\end{cases} \quad (22)$$

where η_{tank} is the fuel tank efficiency; P_e is the engine power; P_{tank} is the fuel tank power; T_{e} is the engine torque; n_e is the engine speed; $Q_{fuel}(t)$ is the fuel rate with the unit of L/s; zd is the heavy gasoline, 7.1 CNY/L; g is the acceleration of gravity; and H_u is the lower heating value of the gasoline, 46000 kJ/kg.

$$\eta_{batt} = \frac{P_m}{P_{batt}} \quad (23)$$

where η_{batt} is the efficiency of motor; and P_{batt} is the battery power.

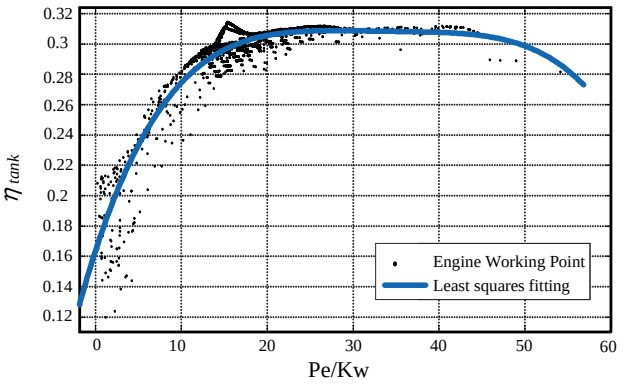

FIGURE 12. The engine working points and fuel tank efficiency.

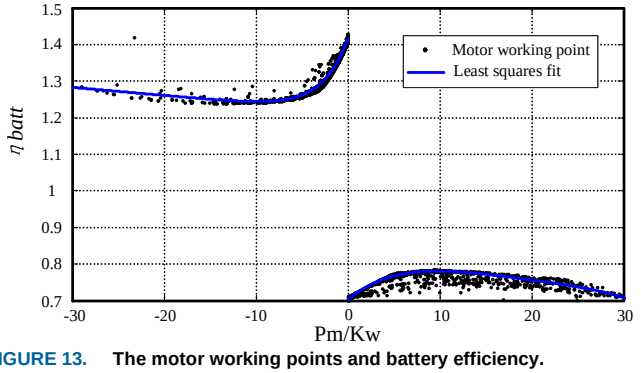

FIGURE 13. The motor working points and battery efficiency.

2) Reduce the control degree-of-freedom from two to one. In this study, the torque distribution and gear decision are taken as control variables and optimization complexity arises due to existence of two parameters. According to the experimental results of global optimization, the distribution law of the optimal gear shifting can be extracted offline and

This article has been accepted for publication in a future issue of this journal, but has not been fully edited. Content may change prior to final publication. Citation information: DOI 10.1109/ACCESS.2019.2933015, IEEE Access

applied in the DP in real time. The optimal gear position distribution extracted from experimental results is shown in Fig. 14, and we can find that the distribution map of the gear position is very clear, and thus the shifting law can be summarized with high efficiency. By this manner, the control degree-of-freedom can be reduced from two to one, and the calculation efficiency is substantially improved.

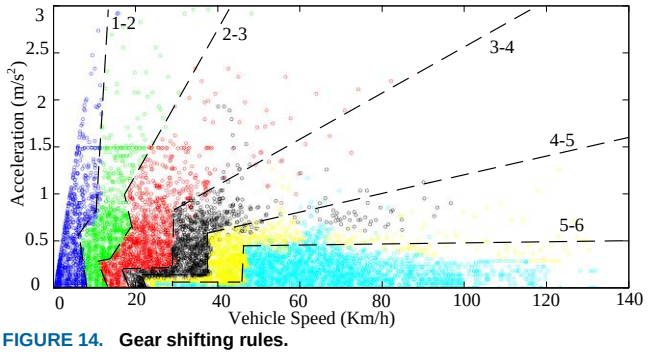

FIGURE 14. Gear shifting rules.

B. ROLLING OPTIMIZATION SOLVED BY THE DP

The energy management of PHEVs within the prediction horizon is a typical nonlinear optimization problem with multi constraints. At step k, the MPC controller computes the energy split between the engine and ISG to minimize the operating cost J_k, which is expressed in (24) along with necessary constraints formulated in (25) and (26).

$$\begin{aligned} J_k &= \sum_{t=k}^{k+p} (L(x(t),u(t)) + \varphi(SOC(t)) \\ &= \sum_{t=k}^{k+p} (\alpha_{fuel} \cdot Q_{fuel}(t) + \alpha_{elec} \cdot P_{bat}(t) + \varphi(SOC(t))) \end{aligned} \tag{24}$$

$$\varphi(SOC(t)) = \begin{cases} 0, SOC(t) \geq SOC_r(t) \\ \alpha(SOC(t) - SOC_r(t))^2, SOC(t) \leq SOC_r(t) \end{cases} \tag{25}$$

$$\begin{cases} SOC_{\min} \leq SOC(t) \leq SOC_{\max} \\ n_{e\_\min} \leq n_e(t) \leq n_{e\_\max} \\ T_{e\_\min}(n_e(t)) \leq T_e(t) \leq T_{e\_\max}(n_e(t)) \\ n_{m\_\min} \leq n_m(t) \leq n_{m\_\max} \\ T_{m\_\min}(n_m(t)) \leq T_m(t) \leq T_{m\_\max}(n_m(t)) \\ T_{req}(t) = T_e(t) + T_m(t) + T_{brake}(t) \\ i_g(t) \in \{1,2,3,\ldots,i_{\max}\} \\ k \leq t \leq k+p \end{cases} \tag{26}$$

where $x(t)$ is the state variable battery SOC; $u(t)$ is the vector of control variables, i.e., the desired output torque of the engine; and $L(x(t),u(t))$ denotes the instantaneous objective function; α_{fuel} expresses the price of the fuel, and equals 7.2 CNY/L; $Q_{fuel}(t)$ is the fuel rate with unit of L/s; α_{elec} represents the price of electricity, i.e., 0.52 CNY/*KWh*; and $P_{bat}(t)$ denotes the battery power. The subscripts min and max are the minimum and maximum bounded values of each variable; α is a penalty coefficient; and $\varphi(SOC(t))$ is the penalty function trying to converge the SOC to the setting value. $n_e(k)$ and $n_m(k)$ represent the speed of the engine and motor, respectively; $T_{brake}(k)$ denotes the mechanical braking torque; i_g is the gear number; and T_e, T_m and T_{req} express the torque of the engine, motor and road demand, respectively. According to (24)-(26), the optimization procedure is a typical nonlinear multistep decision problem, which can be generally solved by the DP. The optimal control sequence $u^* = \{u_k^*, u_{k+1}^*, u_{k+2}^*, \cdots, u_{k+p-1}^*\}$ is derived from minimization of the cost function in the horizon, as

$$J^* = \min\left[\sum_{t=k}^{k+p} (L(x(t),u^*(t)) + \varphi(x(t)))\right] \tag{27}$$

At step $k+i$ $(0 \leq i \leq p-1)$, the sub-problem is solved by the Bellman optimal principle, as

$$\begin{cases} J^*(x(k+i)) = \min[L(x(k+i),u(k+i)) + J^*(x(k+i+1))] \\ J^*(x(k+p)) = \min[L(x(k+p),u(k+p)) + \varphi(x(k+p))] \end{cases} \tag{28}$$

where $J^*(x(k+i))$ is the optimal cost function vector changing from step $k+i$ to $k+p$ at state $x(k+i)$; $x(k+i+1)$ is the state transferring from $x(k+i)$ with the control variable $u(k+i)$.

To summarize, the whole control framework of the MPC algorithm is built considering the above discussed three aspects: 1) the short-term speed prediction considering the traffic information, 2) the fast SOC reference generation based on the DP, and 3) the rolling optimization. The whole control flowchart is depicted in Fig. 15.

In next step, simulations are conducted, and discussions are performed to demonstrate advances of the proposed control framework.

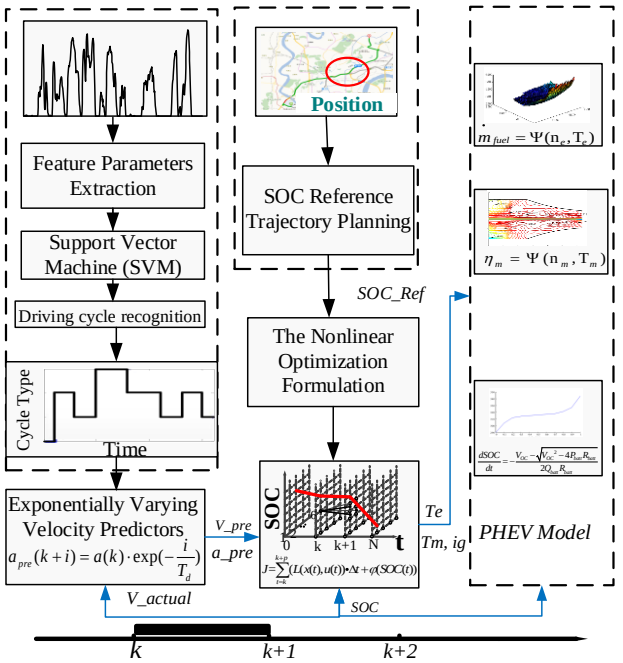

FIGURE 15. The system control flowchart.

This article has been accepted for publication in a future issue of this journal, but has not been fully edited. Content may change prior to final publication. Citation information: DOI 10.1109/ACCESS.2019.2933015, IEEE Access

VI. SIMULATION AND DISCUSSIONS

To evaluate performance of the proposed algorithm, two cases are studied. First, two algorithms are leveraged to construct the SOC reference trajectory for application of the MPC algorithm m. One algorithm is the proposed fast DP algorithm and the other one is a simple linear algorithm that only correlates with the trip duration. The main destination is to examine the cost improvement when generating the SOC reference with consideration of the traffic information. Based on different planned SOC trajectories, the MPC is conducted to compare the induced savings of the operating cost. Second, the MPC algorithm should consider the updating frequency of the traffic information, hence, simulations with different updating frequencies are conducted to find the optimal frequency. Meanwhile, the DP is applied as an offline optimal benchmark to quantify the detailed savings of the operating cost. In this study, a real driving cycle is presented in Fig. 16, and its length is 26.07 Km, which is beyond the AER when the initial battery SOC is 0.5. Certainly, the engine needs to participate in driving the vehicle.

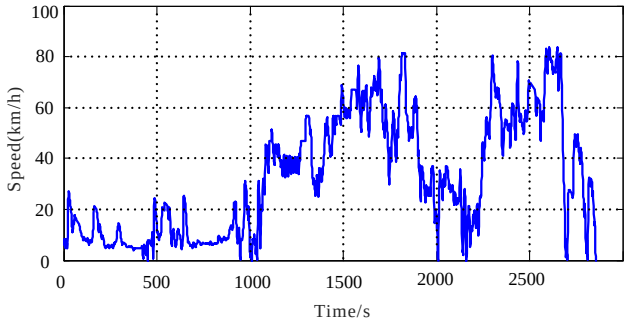

FIGURE 16. The acquired driving cycle for validation.

A. PERFORMANCE COMPARISON OF MPC WITH AND WITHOUT TRAFFIC INFORMATION

The trip duration is assumed to be known without help of traffic information and a simple SOC reference trajectory is defined to decrease linearly from the initial maximum SOC to the minimum threshold, thus we can attain

$$SOC_r(k) = SOC_0 - \frac{t(k)}{t_{cyc}}(SOC_0 - SOC_{\min}) \qquad (29)$$

where t_{cyc} is the duration of whole trip and $SOC_r(k)$ denotes the SOC reference at step k. The MPC algorithms with detailed traffic information and only with the trip duration as well as the DP algorithm are implemented under the actual driving cycle, corresponding SOC trajectories and total operation costs are shown in Figs. 15 and 16, respectively.

In the beginning of the trip, the vehicle speed is low in the urban congested condition. No matter the SOC reference is determined based on the real-time traffic information or trip duration, the vehicle is mostly under the pure electric mode to prevent the engine from working in low efficiency area. The SOC reference generated from the real-time information is shown in the black line depicted in Fig. 17, which is updated every 200 s. As can be found, the decreasing slope of the SOC trajectory based on the MPC with transportation information is similar to that based on the DP. Due to the step update of the traffic environment, depicted in the circle, the SOC reference trajectory based on the traffic information planning imports some gaps. As can be found in BOX1, compared to the SOC reference with knowing the driving duration, the SOC reference based on the traffic information can avoid excessive discharge of the battery, and looks similar to that based on DP. In BOX2, the road demand power is larger than before, and the linear SOC reference means that the battery cannot release enough electric power to driving the vehicle. As such, the engine needs to start and participate in supplementing the extra power. Obviously, it is not an optimal solution. It is important to note that the acquired traffic flow speed differs from the actual vehicle velocity, and thus certain deviation among the generated SOC reference curves exists. As a result, the built MPC algorithm cannot reach the fuel optimality of the DP. As illustrated in Table IV, the MPC based on real-time traffic information can reach 92.83% of the fuel economy of the DP, which is 6.18% higher than that with only knowing the trip duration. The time consumption is around 0.037 s per step when the DP is applied to resolve the global optimal control, and the MPC strategy only needs 0.039 s to 0.041 s in each step. Although the calculation intensity based on the DP is shorter than that based on MPC, the DP needs to search the optimal solution inversely for the whole driving cycle of 2856 s, suggesting the infeasibility of real-time application.

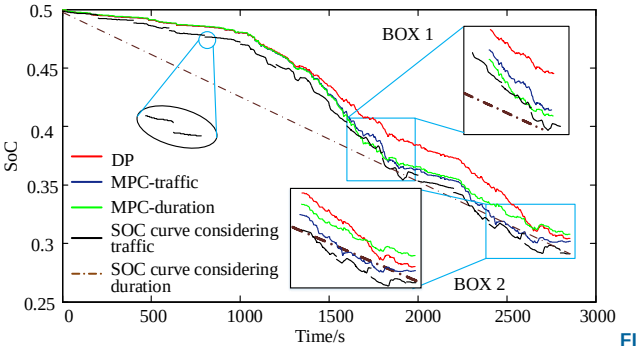

GURE 17. SOC trajectory of DP and MPC with traffic information and trip duration.

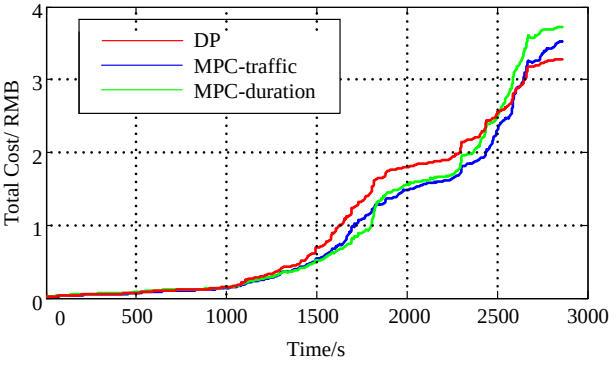

FIGURE 18. Total cost of DP and MPC with traffic information or trip duration.

The working properties of the engine when the real-time traffic information is obtained during driving is shown in Fig. 19, from which it can be observed that the operating points of

This article has been accepted for publication in a future issue of this journal, but has not been fully edited. Content may change prior to final publication. Citation information: DOI 10.1109/ACCESS.2019.2933015, IEEE Access

the engine based on the DP strategy mostly locate in a higher efficiency area. The overall operating efficiency based on the MPC with the traffic information is lower than that of the DP, and the MPC only with the duration performs worst.

TABLE IV
SIMULATION RESULTS COMPARISON

	MPC-traffic	MPC-duration	DP
Total Cost/ RMB	3.5103	3.7127	3.2753
Fuel economy	92.83%	86.65%	100%
Initial SOC	0.5	0.5	0.5
Terminal SOC	0.3018	0.3079	0.3043
Calculation time/s	112	115	108

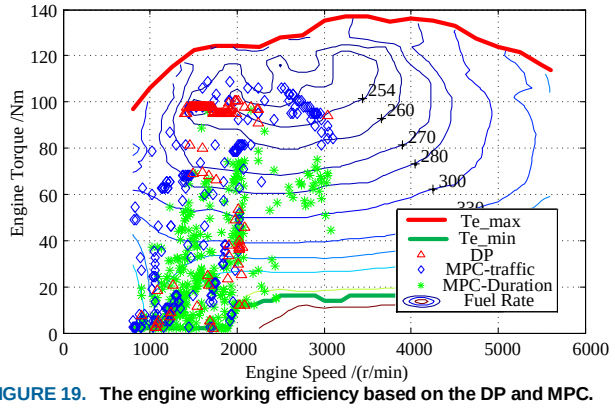

FIGURE 19. The engine working efficiency based on the DP and MPC.

B. Comparison of MPC with Traffic Information Updated by Different Frequencies

The target vehicle can update the transportation information every 200 s. The first three speed profiles reflecting the target mileage generated from the traffic simulation environment is presented in Fig. 20. As can be seen, the varying tendency of the traffic speed is basically coincident with the actual value.

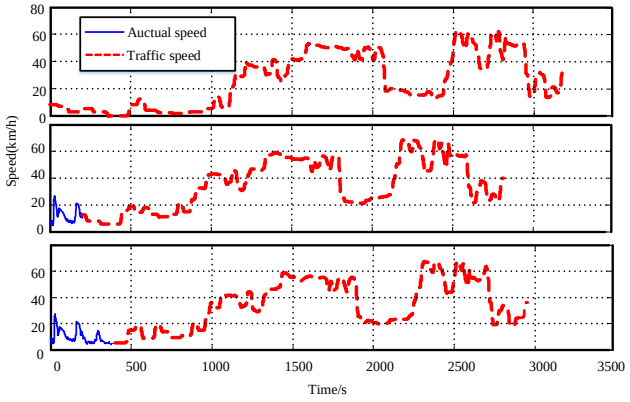

FIGURE 20. The updated traffic driving cycle.

To compare the savings, the MPC algorithms with static traffic information and with update frequencies of 200 s, 400 s, 600 s, and 800 s are respectively applied. Detailed results are shown in Figs. 21 and 22. Here, the MPC-static means the traffic information is obtained only once at the start of trip and not updated for the rest time. The MPC-200, MPC-400, MPC-600 and MPC-800 mean the average traffic flow speed is assumed to be updated every 200 s, 400 s, 600 s and 800 s, respectively. In the beginning of the trip, the current traffic is relatively congested, and the algorithm predicts that the vehicle would take more time to finish the trip. As such, the SOC decreases with slower speed. After 1000 s, the vehicle speed becomes higher, and then the battery participates in driving the vehicle with more power, leading to faster decrement of the SOC. The total costs of the DP and MPC with different updating frequencies are shown are Fig. 20. It can be found that the predicted duration is more than the actual duration and the SOC reference generated by the initially updated traffic speed cannot be used up for a whole trip. As a result, the terminal SOC of the MPC-static cannot reach the low SOC threshold, leading to higher fuel economy. As shown in Table V, the total operating cost is minimal when the real-time traffic information is updated every 200 s. The MPC with the traffic information tends to attain less fuel cost with increase of the updating frequency. Certainly, the timely update of the traffic information can be beneficial for improvement of the controlling performance of the proposed strategy.

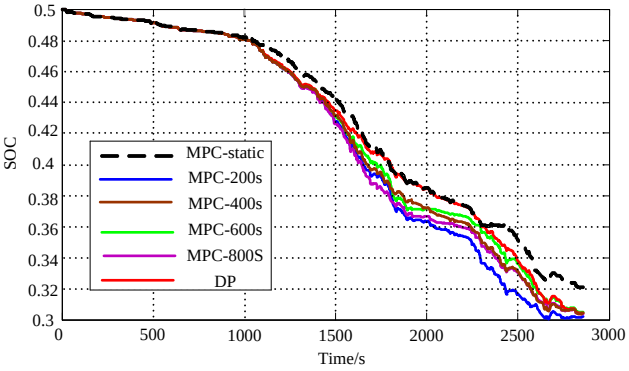

FIGURE 21. SOC trajectory of DP and MPC with different traffic information.

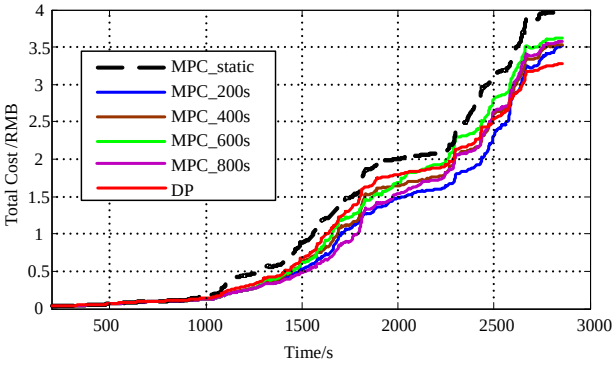

FIGURE 22. Total cost of DP and MPC with different updating cycles.

TABLE V
RESULTS OF DP AND MPC WITH DIFFERENT TRAFFIC INFORMATION

	Total Cost/ RMB	Optimality	Terminal SOC
MPC-static	3.9767	78.95%	0.3211
MPC-200	3.5103	92.83%	0.3043
MPC-400	3.5353	92.06%	0.3041
MPC-600	3.619	89.51%	0.3049
MPC-800	3.5713	90.96%	0.3040
DP	3.2753	100%	0.3043

This article has been accepted for publication in a future issue of this journal, but has not been fully edited. Content may change prior to final publication. Citation information: DOI 10.1109/ACCESS.2019.2933015, IEEE Access

VII. CONCLUSION

In this paper, a trip-oriented predictive energy management strategy is proposed to realize near-optimal energy distribution of the PHEV. An exponentially varying prediction model, which can be applied in all driving conditions, is put forward based on a tunable decay coefficient regulated by the SVM, thus improving adaptability to different driving conditions. According to the acquired traffic information, a virtual traffic simulation environment is established to model the vehicle driving path and updated with real-time traffic data. The DP algorithm is proposed to plan the SOC reference trajectory with fast calculation speed by simplifying the powertrain model and to conduct the short-term rolling optimization in the MPC framework. The operating economy of the MPC with or without traffic information is analyzed and compared. On this basis, the impact of different update frequency on operating cost is evaluated. Simulation results reveal that the proposed predictive algorithm is capable of achieving superior operating cost economy and tends to perform better with decrement of the update frequency of the traffic information, proving feasibility of the whole control framework.

Next step will be focused on more detailed analysis in terms of update frequency of the traffic information. In addition, the real vehicle test will be conducted to further investigate the effectiveness of the proposed algorithm.

REFERENCES

[1] B. Mashadi and D. Crolla, *Hybrid Electric Vehicles*. 2011.
[2] C. Mi, M. A. Masrur, and D. W. Gao, *Plug-in Hybrid Electric Vehicles*. 2017.
[3] W. Enang and C. Bannister, "Modelling and control of hybrid electric vehicles (A comprehensive review)," *Renewable & Sustainable Energy Reviews*, vol. 74, pp. 1210-1239, 2017.
[4] V. Krithika and C. Subramani, "A comprehensive review on choice of hybrid vehicles and power converters, control strategies for hybrid electric vehicles," *International Journal of Energy Research*, vol. 42, no. 1, 2017.
[5] R. Xiong, J. Cao, and Q. Yu, "Reinforcement learning-based real-time power management for hybrid energy storage system in the plug-in hybrid electric vehicle," *Applied Energy*, vol. 211, pp. 538-548, 2018.
[6] C. M. Martinez, X. Hu, D. Cao, E. Velenis, B. Gao, and M. Wellers, "Energy Management in Plug-in Hybrid Electric Vehicles: Recent Progress and a Connected Vehicles Perspective," *IEEE Transactions on Vehicular Technology*, vol. 66, no. 6, pp. 4534-4549, 2017.
[7] S. Onori, L. Serrao, and G. Rizzoni, "Hybrid electric vehicles : energy management strategies," *Encyclopedia of Energy*, vol. 277, no. 4, pp. 197-213, 2016.
[8] S. G. Li, S. M. Sharkh, F. C. Walsh, and C. N. Zhang, "Energy and Battery Management of a Plug-In Series Hybrid Electric Vehicle Using Fuzzy Logic," *IEEE Transactions on Vehicular Technology*, vol. 60, no. 8, pp. 3571-3585, 2011.
[9] S. G. Wirasingha and A. Emadi, "Classification and Review of Control Strategies for Plug-In Hybrid Electric Vehicles," *IEEE Transactions on Vehicular Technology*, vol. 60, no. 1, pp. 111-122, 2011.
[10] S. A. Zulkifli, N. Saad, and A. R. A. Aziz, "Deterministic and Fuzzy Logic Control of Split-Parallel Through-the-Road Hybrid Electric Vehicle," in *International Conference on Computer*, 2016.
[11] B. M. Duan, Q. N. Wang, J. N. Wang, X. N. Li, and T. Ba, "Calibration efficiency improvement of rule-based energy management system for a plug-in hybrid electric vehicle," *International Journal of Automotive Technology*, vol. 18, no. 2, pp. 335-344, 2017.
[12] S. Stockar, V. Marano, M. Canova, G. Rizzoni, and L. Guzzella, "Energy-Optimal Control of Plug-in Hybrid Electric Vehicles for Real-World Driving Cycles," *IEEE Transactions on Vehicular Technology*, vol. 60, no. 7, pp. 2949-2962, 2011.
[13] C. Xiang, F. Ding, W. Wang, and W. He, "Energy management of a dual-mode power-split hybrid electric vehicle based on velocity prediction and nonlinear model predictive control," *Applied Energy*, vol. 189, pp. 640-653, 2017.
[14] V. Ngo, T. Hofman, M. Steinbuch, and A. Serrarens, "Optimal Control of the Gearshift Command for Hybrid Electric Vehicles," *IEEE Transactions on Vehicular Technology*, vol. 61, no. 8, pp. 3531-3543, 2012.
[15] S. Xie, F. Sun, H. He, and J. Peng, "Plug-In Hybrid Electric Bus Energy Management Based on Dynamic Programming," *Energy Procedia*, vol. 104, pp. 378-383, 2016.
[16] Y. Yang, X. Hu, H. Pei, and Z. Peng, "Comparison of power-split and parallel hybrid powertrain architectures with a single electric machine: Dynamic programming approach," *Applied Energy*, vol. 168, pp. 683-690, 2016.
[17] B. C. Chen, Y. Y. Wu, and H. C. Tsai, "Design and analysis of power management strategy for range extended electric vehicle using dynamic programming," *Applied Energy*, vol. 113, no. 1, pp. 1764-1774, 2014.
[18] Zheng Chen, C. C. Mi, Jun Xu, Xianzhi Gong, and Chenwen You, "Energy Management for a Power-Split Plug-in Hybrid Electric Vehicle Based on Dynamic Programming and Neural Networks," *IEEE Transactions on Vehicular Technology*, vol. 63, no. 4, pp. 1567-1580, 2014.
[19] N. Kim, S. Cha, and H. Peng, "Optimal Control of Hybrid Electric Vehicles Based on Pontryagin's Minimum Principle," *IEEE Transactions on Control Systems Technology*, vol. 19, no. 5, pp. 1279-1287, 2011.
[20] C. Zheng, G. Xu, K. Xu, Z. Pan, and Q. Liang, "An energy management approach of hybrid vehicles using traffic preview information for energy saving," *Energy Conversion and Management*, vol. 105, pp. 462-470, 2015.
[21] Y. Xie, A. Savvaris, and A. Tsourdos, "Fuzzy logic based equivalent consumption optimization of a hybrid electric propulsion system for unmanned aerial vehicles," *Aerospace Science and Technology*, vol. 85, pp. 13-23, 2019.
[22] F. Odeim, J. Roes, L. Wülbeck, and A. Heinzel, "Power management optimization of fuel cell/battery hybrid vehicles with experimental validation," *Journal of Power Sources*, vol. 252, pp. 333-343, 2014.
[23] H. Tian, X. Wang, Z. Lu, Y. Huang, and G. Tian, "Adaptive Fuzzy Logic Energy Management Strategy Based on Reasonable SOC Reference Curve for Online Control of Plug-in Hybrid Electric City Bus," *IEEE Transactions on Intelligent Transportation Systems*, vol. 19, no. 5, pp. 1607-1617, 2018.
[24] R. Xiong, Y. Zhang, H. He, X. Zhou, and M. G. Pecht, "A Double-Scale, Particle-Filtering, Energy State Prediction Algorithm for Lithium-Ion Batteries," *IEEE Transactions on Industrial Electronics*, vol. 65, no. 2, pp. 1526-1538, 2018.
[25] C. Zheng, W. Li, and Q. Liang, "An Energy Management Strategy of Hybrid Energy Storage Systems for Electric Vehicle Applications," *IEEE Transactions on Sustainable Energy*, vol. 9, no. 4, pp. 1880-1888, 2018.
[26] S. Uebel, N. Murgovski, C. Tempelhahn, and B. Baker, "Optimal Energy Management and Velocity Control of Hybrid Electric Vehicles," *IEEE Transactions on Vehicular Technology*, vol. 67, no. 1, pp. 327-337, 2018.
[27] N. Bizon, "Real-time optimization strategies of Fuel Cell Hybrid Power Systems based on Load-following control: A new strategy, and a comparative study of topologies and fuel economy obtained," *Applied Energy*, vol. 241, pp. 444-460, 2019.
[28] J. Peng, H. He, and R. Xiong, "Rule based energy management strategy for a series–parallel plug-in hybrid electric bus optimized by dynamic programming," *Applied Energy*, vol. 185, pp. 1633-1643, 2017.
[29] Z. Pei, F. Yan, and C. Du, "A comprehensive analysis of energy management strategies for hybrid electric vehicles based on bibliometrics," *Renewable & Sustainable Energy Reviews*, vol. 48, pp. 88-104, 2015.

[30] C. Sun, F. Sun, and H. He, "Investigating adaptive-ECMS with velocity forecast ability for hybrid electric vehicles," *Applied Energy*, vol. 185, pp. 1644-1653, 2017.
[31] S. Chao, X. Hu, S. J. Moura, and F. Sun, "Velocity Predictors for Predictive Energy Management in Hybrid Electric Vehicles," *IEEE Transactions on Control Systems Technology*, vol. 23, no. 3, pp. 1197-1204, 2015.
[32] W. Shabbir and S. A. Evangelou, "Threshold-changing control strategy for series hybrid electric vehicles," *Applied Energy*, vol. 235, pp. 761-775, 2019.
[33] J. Wang, J. Wang, Q. Wang, and X. Zeng, "Control rules extraction and parameters optimization of energy management for bus series-parallel AMT hybrid powertrain," *Journal of the Franklin Institute*, vol. 355, no. 5, pp. 2283-2312, 2018.
[34] J. Han, D. Kum, and Y. Park, "Synthesis of predictive equivalent consumption minimization strategy for hybrid electric vehicles based on closed-form solution of optimal equivalence factor," *IEEE Transactions on Vehicular Technology*, vol. PP, no. 99, pp. 1-1, 2017.
[35] G. Jinquan, H. Hongwen, P. Jiankun, and Z. Nana, "A novel MPC-based adaptive energy management strategy in plug-in hybrid electric vehicles," *Energy*, vol. 175, pp. 378-392, 2019.
[36] K. D. Nguyen, E. Bideaux, M. T. Pham, and P. le Brusq, "Model Predictive Control Dedicated to an Electrified Auxiliary in HEV/PHEV," *Applied Mechanics & Materials*, vol. 532, pp. 50-57, 2014.
[37] L. Guo, B. Gao, Y. Gao, and H. Chen, "Optimal Energy Management for HEVs in Eco-Driving Applications Using Bi-Level MPC," *IEEE Transactions on Intelligent Transportation Systems*, vol. 18, no. 8, pp. 2153-2162, 2017.
[38] S. East and M. Cannon, "Energy Management in Plug-in Hybrid Electric Vehicles: Convex Optimization Algorithms for Model Predictive Control," 2019.
[39] S. Zhang, Y. Luo, J. Wang, X. Wang, and K. Li, "Predictive Energy Management Strategy for Fully Electric Vehicles Based on Preceding Vehicle Movement," *IEEE Transactions on Intelligent Transportation Systems*, vol. 18, no. 11, pp. 3049-3060, 2017.
[40] P. Golchoubian and N. L. Azad, "Real-Time Nonlinear Model Predictive Control of a Battery–Supercapacitor Hybrid Energy Storage System in Electric Vehicles," *IEEE Transactions on Vehicular Technology*, vol. 66, no. 11, pp. 9678-9688, 2017.
[41] X. Li, L. Han, H. Liu, W. Wang, and C. Xiang, "Real-time optimal energy management strategy for a dual-mode power-split hybrid electric vehicle based on an explicit model predictive control algorithm," *Energy*, vol. 172, pp. 1161-1178, 2019.
[42] J. Shin and M. Sunwoo, "Vehicle Speed Prediction Using a Markov Chain With Speed Constraints," *IEEE Transactions on Intelligent Transportation Systems*, vol. PP, no. 99, pp. 1-11, 2018.
[43] M. Ibrahim, S. Jemei, G. Wimmer, and D. Hissel, "Nonlinear autoregressive neural network in an energy management strategy for battery/ultra-capacitor hybrid electrical vehicles," *Electric Power Systems Research*, vol. 136, pp. 262-269, 2016.
[44] H. Borhan, A. Vahidi, A. M. Phillips, M. L. Kuang, I. V. Kolmanovsky, and S. Di Cairano, "MPC-Based Energy Management of a Power-Split Hybrid Electric Vehicle," *IEEE Transactions on Control Systems Technology*, vol. 20, no. 3, pp. 593-603, 2012.
[45] S. Xie, X. Hu, Z. Xin, and L. Li, "Time-Efficient Stochastic Model Predictive Energy Management for a Plug-In Hybrid Electric Bus With an Adaptive Reference State-of-Charge Advisory," *IEEE Transactions on Vehicular Technology*, vol. 67, no. 7, pp. 5671-5682, 2018.
[46] G. Li, J. Zhang, and H. He, "Battery SOC constraint comparison for predictive energy management of plug-in hybrid electric bus," *Applied Energy*, vol. 194, 2016.
[47] S. Chao, H. Xiaosong, S. J. Moura, and S. Fengchun, "Velocity Predictors for Predictive Energy Management in Hybrid Electric Vehicles," *IEEE Transactions on Control Systems Technology*, vol. 23, no. 3, pp. 1197-1204, 2015.
[48] S. Di Cairano, D. Bernardini, A. Bemporad, and I. V. Kolmanovsky, "Stochastic MPC With Learning for Driver-Predictive Vehicle Control and its Application to HEV Energy Management," *IEEE Transactions on Control Systems Technology*, vol. 22, no. 3, pp. 1018-1031, 2014.
[49] H. He, J. Cao, and J. Peng, "Online Prediction with Variable Horizon for Vehicle's Future Driving-Cycle," *Energy Procedia*, vol. 105, pp. 2348-2353, 2017.
[50] Y. Zhou, A. Ravey, and M.-C. Péra, "A survey on driving prediction techniques for predictive energy management of plug-in hybrid electric vehicles," *Journal of Power Sources*, vol. 412, pp. 480-495, 2019.
[51] Y. Huang, H. Wang, A. Khajepour, H. He, and J. Ji, "Model predictive control power management strategies for HEVs: A review," *Journal of Power Sources*, vol. 341, pp. 91-106, 2017.
[52] H. A. Borhan, A. Vahidi, A. M. Phillips, M. L. Kuang, and I. V. Kolmanovsky, "Predictive Energy Management of a Power-Split Hybrid Electric Vehicle," in *American Control Conference*, 2009.
[53] S. Zhang, R. Xiong, and F. Sun, "Model predictive control for power management in a plug-in hybrid electric vehicle with a hybrid energy storage system," *Applied Energy*, vol. 185, pp. 1654-1662, 2017.
[54] H. Borhan, A. Vahidi, A. M. Phillips, M. L. Kuang, I. V. Kolmanovsky, and S. D. Cairano, "MPC-Based Energy Management of a Power-Split Hybrid Electric Vehicle," *IEEE Transactions on Control Systems Technology*, vol. 20, no. 3, pp. 593-603, 2012.
[55] H. He, J. Guo, J. Peng, H. Tan, and S. Chao, "Real-time global driving cycle construction and the application to economy driving pro system in plug-in hybrid electric vehicles," *Energy*, vol. 152, 2018.
[56] Y. Liu, J. Li, Z. Chen, D. Qin, and Y. Zhang, "Research on a multi-objective hierarchical prediction energy management strategy for range extended fuel cell vehicles," *Journal of Power Sources*, vol. 429, pp. 55-66, 2019.
[57] M. Montazeri-Gh and Z. Pourbafarani, "Near-Optimal SOC Trajectory for Traffic-Based Adaptive PHEV Control Strategy," *IEEE Transactions on Vehicular Technology*, vol. 66, no. 11, pp. 9753-9760, 2017.
[58] H. He, J. Zhang, and G. Li, "Model Predictive Control for Energy Management of a Plug-in Hybrid Electric Bus ☆," *Energy Procedia*, vol. 88, pp. 901-907, 2016.
[59] S. Xie *et al.*, "Model predictive energy management for plug-in hybrid electric vehicles considering optimal battery depth of discharge," *Energy*, vol. 173, pp. 667-678, 2019.
[60] S. Xie, X. Hu, Z. Xin, and J. Brighton, "Pontryagin's Minimum Principle based model predictive control of energy management for a plug-in hybrid electric bus," *Applied Energy*, vol. 236, pp. 893-905, 2019.
[61] S. Chao, S. J. Moura, X. Hu, J. K. Hedrick, and F. Sun, "Dynamic Traffic Feedback Data Enabled Energy Management in Plug-in Hybrid Electric Vehicles," *IEEE Transactions on Control Systems Technology*, vol. 23, no. 3, pp. 1075-1086, 2015.
[62] H. Hongwen, G. Jinquan, P. Jiankun, T. Huachun, and S. Chao, "Real-time global driving cycle construction and the application to economy driving pro system in plug-in hybrid electric vehicles," *Energy*, vol. 152, pp. 95-107, 2018.
[63] H. He, J. Guo, N. Zhou, C. Sun, and J. Peng, "Freeway Driving Cycle Construction Based on Real-Time Traffic Information and Global Optimal Energy Management for Plug-In Hybrid Electric Vehicles," *Energies*, vol. 10, no. 11, p. 1796, 2017.
[64] J. Lian *et al.*, "A Mixed Logical Dynamical-Model Predictive Control (MLD-MPC) Energy Management Control Strategy for Plug-in Hybrid Electric Vehicles (PHEVs)," *Energies*, vol. 10, no. 1, p. 74, 2017.
[65] H. Xi, T. Ying, and X. He, "An intelligent multi-feature statistical approach for discrimination of driving conditions of hybrid electric vehicle," *IEEE Transactions on Intelligent Transportation Systems*, vol. 12, no. 2, pp. 453-465, 2011.
[66] Z. Lei, D. Cheng, Y. Liu, D. Qin, Y. Zhang, and Q. Xie, "A Dynamic Control Strategy for Hybrid Electric Vehicles Based on Parameter Optimization for Multiple Driving Cycles and Driving Pattern Recognition," *Energies*, vol. 10, no. 1, p. 54, 2017.
[67] ZULKEFLI, M. A. Mohd, J. Zheng, Z. Sun, LIU, and X. Henry, "Hybrid powertrain optimization with trajectory prediction based on inter-vehicle-communication and vehicle-infrastructure-integration," *Transportation Research Part C*, vol. 45, no. 9, pp. 41-63, 2014.